

1 “Neighbourhood watch” model: embryonic epiblast cells assess positional information in 2 relation to their neighbours

- 3
- 4 • Running title: **Neighbourhood watch model**

5
6 Hyung Chul Lee^{1†}, Cato Hastings^{1†}, Nidia M.M. Oliveira¹, Rubén Pérez-Carrasco², Karen M.
7 Page³, Lewis Wolpert^{1‡} and Claudio D. Stern^{1*}

8
9 ¹Department of Cell and Developmental Biology, University College London, Gower
10 Street, London WC1E 6BT, UK.

11 ²Department of Life Sciences, Imperial College London, South Kensington Campus,
12 London SW7 2AZ, U.K.

13 ³Department of Mathematics, University College London, Gower Street, London WC1E
14 6BT, U.K.

15 † These authors contributed equally.

16 ‡ Deceased 28 Jan 2021

17 * correspondence to: c.stern@ucl.ac.uk

18
19 **Keywords:** morphogen, chick embryo, polarity, primitive streak, gastrulation, cell
20 communication, SMAD

21
22 **Summary statement:** In a large developing system, the chick embryo before gastrulation, cells
23 interpret gradients of positional signals relative to their neighbours to position the primitive
24 streak, establishing bilateral symmetry.

25 26 **Abstract**

27 In many developing and regenerating systems, tissue pattern is established through
28 gradients of informative morphogens, but we know little about how cells interpret these.
29 Using experimental manipulation of early chick embryos including misexpression of an
30 inducer (VG1 or ACTIVIN) and an inhibitor (BMP4), we test two alternative models for
31 their ability to explain how the site of primitive streak formation is positioned relative to
32 the rest of the embryo. In one model, cells read morphogen concentrations cell-
33 autonomously. In the other, cells sense changes in morphogen status relative to their
34 neighbourhood. We find that only the latter model can account for the experimental
35 results, including some counter-intuitive predictions. This mechanism (which we name
36 “neighbourhood watch” model) illuminates the classic “French Flag Problem” and how
37 positional information is interpreted by a sheet of cells in a large developing system.
38
39

40 **Introduction**

41 In the late 1960s, Lewis Wolpert introduced the concept of “positional information”,
42 asking the question of how cells within a morphogenetic field could adopt several cell-
43 type identities in response to signalling cues from the embryo. The analogy of a French
44 flag, with three colours: red, white and blue, was used to symbolise the cell types
45 (Wolpert, 1968, Wolpert, 1969). Wolpert proposed that a gradient of a hypothetical
46 “morphogen” diffusing away from a local source and decaying with distance would be

47 read by cells, which respond with discrete thresholds to adopt the various identities. He
48 named this the “French Flag problem”.

49 Since, several systems have been found in which a morphogen imparts positional
50 information resulting in a defined morphological pattern. These include head and foot
51 formation in Hydra (Schaller, 1973, Bode, 2011), patterning of the wing (Lecuit et al.,
52 1996), leg and antenna imaginal discs of the fly (Postlethwait and Schneiderman, 1971)
53 and limb regeneration in vertebrates (Kumar et al., 2007). Various mechanisms have been
54 studied by which cells might interpret such morphogen gradients so that their positions are
55 defined precisely and robustly. In cultured cells and explant systems (Gurdon et al., 1999,
56 Gurdon et al., 1995) it has been shown that cells respond directly to morphogen
57 concentration, in a manner most similar to that described by Wolpert (Wolpert, 1969). In
58 vertebrate neural tube patterning, the gradient of Shh is transformed into a dynamic profile
59 of Gli (a transcription factor) to generate spatial patterns of downstream gene expression,
60 suggesting that cells interpret positional information using intracellular regulatory
61 networks, where a temporal element is important (Dessaud et al., 2010, Cohen et al.,
62 2013). The *bicoid* gradient, which sets up the anterior–posterior axis in fruit fly embryos
63 has been studied extensively (Driever and Nusslein-Volhard, 1988b, Driever and
64 Nusslein-Volhard, 1988a, Gregor et al., 2007b, Gregor et al., 2007a) and it has been
65 suggested that spatial averaging across nuclei is one mechanism by which noise is reduced
66 in the transduction of the *bicoid* signal (Gregor et al., 2007a).

67 All the above systems are relatively small (<100 cell diameters) (Wolpert, 1969) allowing
68 stable gradients to be set up which span the entire field. However, some developing
69 systems are much larger in size, begging the question of what mechanisms cells might use
70 to assess their positions. An example of such a large system is the early chick embryo just
71 before the onset of gastrulation. The embryo contains as many as 20,000-50,000 cells and
72 is approximately 3mm in diameter. Within this large field the primitive streak, the site of
73 gastrulation, can arise at any point around the circumference. Any isolated fragment of
74 this large embryo can initiate primitive streak formation; however, only one primitive
75 streak forms, suggesting the existence of patterning events that coordinate cell behaviours
76 across the whole field.

77 In these early embryos, the “pattern” is established in the marginal zone, a ring-like region
78 of extraembryonic tissue, lying just outside of the central disk-like area pellucida, where
79 the embryo will arise. The primitive streak, the first indication of the future midline of the
80 embryo, arises at one edge of the inner area pellucida, adjacent to the posterior part of the
81 marginal zone, where the TGF β -related signalling molecule cVG1 is expressed. Previous
82 studies have shown that positioning of the primitive streak requires “positive” inducing
83 signals by cVG1/NODAL from the posterior marginal zone near the site of streak
84 formation, and that this is antagonised by BMP signalling which is highest at the opposite
85 (anterior) end of the blastoderm (Fig. S1A) (Shah et al., 1997, Streit et al., 1998,
86 Bertocchini and Stern, 2012, Streit and Stern, 1999, Bertocchini and Stern, 2002, Skromne
87 and Stern, 2002, Bertocchini et al., 2004). The distance between the two extremes of the
88 marginal zone is approximately 300 cell diameters. Previous studies suggested that these
89 signals are part of a “global positioning system” to establish polarity in the chick embryo,
90 (Bertocchini and Stern, 2012, Arias et al., 2017), and therefore that the whole embryo is a
91 coordinated system of positional information.

92 To find out how cells interpret morphogen concentrations to generate positional
93 information, we designed two computational models to represent respectively a fixed
94 gradient, read locally by cells, or a system where cells compare themselves to their
95 neighbours to determine their position in the field. Using a combination of embryological
96 manipulations and computational modelling, we ask which of these two models can best
97 account for the results of various manipulations in the spatial distribution, and intensity of
98 the inducing (cVG1/NODAL) and inhibitory (BMP) signals. We find that the “positional
99 information” that determines the site of primitive streak formation is explained better by a
100 mechanism by which cells compare themselves to their neighbours rather than by a cell
101 autonomous assessment of gradients. We name this the “neighbourhood watch” model.

102

103

104 Results

105 Epiblast cells may sense local differences in strength of inducing signal rather than 106 the absolute amount of inducer

107 When a small pellet of cVG1-expressing cells (HEK293T cells transfected with a cVG1-
108 expression construct) is grafted into the anterior marginal zone (the innermost
109 extraembryonic epiblast, just outside the central embryonic area pellucida), it can initiate
110 formation of an ectopic primitive streak that eventually develops into a full embryonic
111 axis (Shah et al., 1997, Skromne and Stern, 2002). However endogenous *cVG1* mRNA is
112 expressed as a crescent encompassing an arc of about 60° in the posterior marginal zone
113 (Fig. S1A). To mimic this distribution more closely, as well as to test the effects of greater
114 concentration of cVG1 inducing signal, we placed two cVG1-expressing cell pellets side-
115 by-side in the anterior marginal zone, and assessed primitive streak formation by in situ
116 hybridisation for expression of *BRACHYURY* (*cBRA*, =*TBXT*) after overnight culture (Fig.
117 1 A-D). Only a single ectopic primitive streak was generated near the middle of the two
118 cVG1 pellets (Fig. 1 B); neither double nor thicker ectopic streaks were observed, similar
119 to the effects of implanting a single pellet.

120 To provide a stronger and wider signal, we tested the effect of implanting four cVG1-
121 expressing cell pellets side-by-side in the anterior marginal zone. Surprisingly, in the
122 majority of cases (11/16 embryos), no ectopic primitive streak formed and no ectopic
123 *cBRA* expression was seen (Fig. 1 E, H, K). Since application of the equivalent of a quad-
124 dose of inducer spread over a four-fold wider area does not cause either more efficient or
125 wider induction than a single dose, we speculated that “boundaries” to the signalling
126 domain may be required. To test this, we placed a control cell pellet (HEK293T cells
127 transfected with pCA β -GFP; see Methods) to split four cVG1-expressing cell pellets into
128 two groups on either side. The incidence of ectopic streak formation doubled (Fig. 1 F, I,
129 K). If a boundary is indeed important, we might expect that, perhaps paradoxically,
130 ectopic streak induction might increase if a pellet expressing the inhibitor BMP4 (rather
131 than a control pellet) is used to interrupt the set of four cVG1-expressing cell pellets. This
132 is indeed the case (Fig. 1 G, J, K). Together, these results suggest that cells may sense
133 variations in signal strength in relation to their neighbours, rather than measuring the
134 absolute amount of local signal they receive, to determine the outcome of the inductive
135 event.

136 The above experiments were done using pellets of transfected cells, as in previous studies
137 (Bertocchini et al., 2004, Bertocchini and Stern, 2012, Shah et al., 1997, Skromne and
138 Stern, 2002, Streit et al., 1998, Torlopp et al., 2014). One problem with this approach is
139 that cells are likely to express other (unknown) factors that could influence the outcome of
140 the signalling event. Another problem is that these pellets are relatively large (500-1000
141 cells). We therefore decided to substitute the use of cell pellets with protein-soaked
142 microbeads (about 100 μ m diameter). As neither VG1 nor NODAL are available as pure
143 proteins, we decided to use ACTIVIN instead, which can induce axial structures and
144 mesendodermal markers in chick epiblast (Mitrani et al., 1990, Stern et al., 1995). As
145 shown in amphibian animal cap ectoderm explants (Green and Smith, 1990), ACTIVIN
146 also acts through the SMAD 2/3 pathway and generates finely graded responses of

147 mesendoderm induction to different concentrations (Stern et al., 1995). BMP4-soaked
148 beads were used as a source of inhibitory signal. First, we checked if a single soaked bead
149 can mimic the effects of a single cell pellet (Fig. S2). Grafting a bead soaked in ACTIVIN
150 into the anterior marginal zone has the same effect as a cell pellet placed in the same
151 position: it induces an ectopic *cBRA*-expressing primitive streak in adjacent epiblast (Fig.
152 S2, A-E). Conversely, placing a bead of the inhibitor BMP4 in the posterior marginal zone
153 results in either displacement of the endogenous primitive streak to a more lateral position,
154 or two primitive streaks, arising either side of the BMP4-bead (Fig. S2, F-J). With a high
155 concentration of BMP4 (50 ng/ μ l) primitive streak formation was abolished in about half
156 of the embryos (Fig. S2J).

157 Next, we mirrored the experiments done with two or more cell pellets but using soaked
158 beads (Fig. 2). After grafting a single ACTIVIN protein-soaked bead flanked by two
159 control beads, 43% of embryos (6/14) had ectopic *cBRA* expression (Fig. 2, B, G, K),
160 while grafting three control beads had no effect (Fig. 2, A, F, K). When three ACTIVIN
161 beads were grafted in a row to expose a wide domain to the inducing signal, the majority
162 of embryos (78%, 7/9) showed no ectopic *cBRA* expression (Fig. 2, C, H, K). When
163 boundaries to the signalling domain were generated either by introducing a BSA-soaked
164 control bead (Fig. 2, D and I) or a BMP4-soaked bead (Fig. 2, E and J) among the
165 ACTIVIN beads, the proportion of embryos with ectopic *cBRA* expression was restored,
166 to 40% (4/10) and 50% (6/12) respectively (Fig. 2 K). Therefore, as with experiments
167 using cell pellets, these results suggest that cells may sense inducing signals relative to
168 their neighbours, rather than the absolute local amount of inducing signal.

169 **Two alternative models**

170 To distinguish between the two alternative mechanisms of how cells might sense their
171 positions (absolute local morphogen concentration or comparison of local signal strength
172 in relation to their neighbourhood), two mathematical models were designed, one for each
173 of these mechanisms, to make experimentally-testable predictions (for details see
174 Materials and Methods). We model the marginal zone as a one-dimensional ring of cells
175 (Fig. 3 A). Positional information is provided by the balance between an inducer
176 (SMAD2/3 activation in response to a VG1/ACTIVIN/NODAL-type signal) and an
177 inhibitor (SMAD 1/5/8 in response to a BMP signal) within each cell (Fig. 3 B). Model A
178 proposes that each cell independently assesses the concentration of morphogens (inducer
179 vs. inhibitor) it receives: when a threshold is exceeded, the cell is triggered to start
180 primitive streak formation. Model B proposes that cells communicate with their
181 neighbours to assess how the streak-inducing signal changes in space: each cell in the ring
182 compares itself with the average signal strength in its neighbourhood to determine whether
183 or not to initiate streak formation (Fig. 3 B).

184 As an initial test of the model comparison method, we asked whether there exist parameter
185 values allowing both models to replicate the experimental results shown in Fig. 2. We
186 automated the search for parameter values using Bayesian computation, which scores
187 values with a 'likelihood function' (Fig. S3). This function quantifies how well the
188 predicted number and position of ectopic streaks match experimental results on a cell-by-
189 cell basis. All parameter values found were checked to verify that they predict the
190 initiation of ectopic primitive streaks in the appropriate locations, qualitatively defining
191 the 'success' of model predictions. The models were run with parameter values

192 maximizing the model success rate and the likelihood score. Fig. 3 C-G summarises the
193 results of these simulations. No set of parameter values was found that allowed Model A
194 to replicate both experimental results, when either one or three beads of inducer were
195 placed in the anterior marginal zone (Fig. 3 C, D). In contrast, Model B successfully
196 predicts that broadening the domain of ectopic inducer reduces the chance of initiating
197 ectopic streak formation (Fig. 3 D).

198 The two models also differ in their ability to portray the effects of placing a bead of
199 inhibitor between two beads of inducer (Fig. 3 E-G). Model A predicts that the presence of
200 the inhibitor will reduce the likelihood of ectopic streaks (Fig. 3 E, F). However, Model B
201 correctly predicts that only low dose of inhibitor increases the chance of forming an
202 ectopic streak (Fig. 3 F, G). The same results were obtained irrespective of whether the
203 sources of inducer and inhibitor were of small diameter (Fig. 3 C-G, to simulate
204 microbeads as in Fig. 2) or wider (Fig. S4, simulating a cell pellet as in Fig. 1).

205 We sought a single set of bead parameters that would allow both models to mimic the
206 experimental findings (Fig. 3 H). However, choosing a single set of bead parameters could
207 act as a constraint, giving an advantage to one of the models. Therefore, we also
208 performed the parameter inference to allow bead parameters to vary for each model
209 independently (Fig 3 I). Strikingly, Model B always outperforms Model A, regardless of
210 whether a single set of parameters is chosen to fit both models, or whether parameter
211 values are optimised for each model separately (Fig. 3 J).

212 **Challenging the models and testing predictions**

213 **a. Decreasing the amount of inhibitor**

214 In both models, cells measure their position by assessing the relative strength of the
215 intracellular downstream effectors of the inducers (VG1/NODAL/ACTIVIN) and
216 inhibitors (BMP). Therefore, decreasing the streak-inhibiting signal alone should induce
217 ectopic primitive streak formation. In this case, both models predict this outcome (Fig. 4 A
218 and B).

219 To test these predictions experimentally, we used dorsomorphin, an inhibitor of BMP
220 signalling (Yu et al., 2008). A dorsomorphin-soaked bead was grafted in the anterior
221 marginal zone (Fig. 4 A). After overnight culture, an ectopic primitive streak (with *cBRA*
222 expression) was seen to arise close to the bead (Fig. 4 C and D). This result is consistent
223 with a previous study showing that a graft of a cell pellet expressing the BMP antagonist
224 CHORDIN in the area pellucida induces an ectopic streak (Streit et al., 1998). When
225 embryos that had been grafted with a dorsomorphin-bead were examined 6 hours after the
226 graft, ectopic expression of *cVG1* mRNA in the area pellucida (*cVG1* expression is an
227 early target of VG1/NODAL signalling; (Skromne and Stern, 2002, Torlopp et al., 2014))
228 was found in the vicinity of the bead (Fig. 4 E and F).

229 **b. Increasing the amount of inhibitor**

230 A more counterintuitive prediction arises when the strength of inhibition by BMP is
231 increased in a region that normally expresses high levels of BMP (Fig. 5 A). The two
232 models predict different outcomes: Model A predicts that increasing BMP signalling in

233 the anterior marginal zone will reduce the chance of ectopic streak formation (Fig. 5 B).
234 Counterintuitively however, Model B predicts that introducing a bead of inhibitor will
235 increase the streak-inducing values in an area adjacent to the bead (bottom, Fig. 5 B).
236 However Model B also suggests that this effect will be small, perhaps insufficient to result
237 in formation of a mature ectopic primitive streak.

238 In embryological experiments in which a BMP4 bead was grafted into the anterior
239 marginal zone, no *cBRA* expression or streak formation was observed after overnight
240 incubation (Fig. 5 C). After short incubation (4.5 h), however, *cVGL* expression was
241 observed in cells surrounding the grafted BMP4 bead in the anterior marginal zone and
242 slightly in the adjacent area pellucida (Fig. 5 D). *cVGL*-expression was absent from cells
243 directly overlying the bead (Fig. 5 F) (see also (Arias et al., 2017)). In addition, the ectopic
244 expression was very weak, only detectable after prolonged chromogenic development of
245 the in situ hybridisation (Fig. 5 D and F). This ectopic expression of *cVGL* in the anterior
246 marginal zone was transient: it was seen at 4.5 h and disappeared by 6 h, remaining mostly
247 in the lower layer of the area opaca (germ wall; Fig. 5 E and G). In conclusion, this
248 experimental result conforms with the predictions of Model B but not those of Model A.

249 c. Effect of adjacent sub-threshold amounts of inducer and inhibitor

250 We have seen that an increase in streak-inhibiting signal can result in paradoxical
251 induction of *cVGL*, which is only predicted by Model B. However, no ectopic *cBRA*
252 expression is observed. If it is indeed the case that cells assess their position in comparison
253 with their neighbours (Model B), rather than measuring the absolute local levels of
254 inducer and inhibitor, then introducing a sub-threshold amount of inducer flanked by low
255 amounts of inhibitor would both deepen and steepen the gradient and might therefore be
256 expected, perhaps paradoxically, to generate a new streak. Model A, in contrast, might
257 predict that neither concentration is high enough locally to affect cell fates resulting in a
258 failure of ectopic streak formation. To simulate this, we explored parameter values for
259 both models that could generate this result (Fig. 6). We find that only Model B can predict
260 the initiation of an ectopic streak (Fig. 6 D-F). No parameters were found that allowed
261 Model A to produce the same result (Fig. 6 D-F).

262 Next, we tested this prediction experimentally. We began by establishing the minimum
263 threshold of ACTIVIN concentration for PS induction; 2.5 ng/ μ l of ACTIVIN does not
264 induce *cBRA* (Fig. S2 D). When two BMP4-beads (6.25 ng/ μ l) were separated by a
265 control bead, no ectopic PS formed (0/9) (Fig. 6 A and G). When an ACTIVIN-bead (2.5
266 ng/ μ l) was flanked by control beads, 97% of embryos showed no ectopic primitive streak
267 (n=37) (Fig. 6 B and H). We then tested the predictions of the model experimentally:
268 when a sub-threshold ACTIVIN bead was flanked by BMP4 beads, *cBRA* expression was
269 seen in 12.5% of cases (n=56) (Fig. 6 C and I). However, a higher concentration of BMP4
270 (12.5 ng/ μ l) in the neighbouring beads reduced the proportion of embryos with an ectopic
271 streak (to 9%; n=22) (data not shown), suggesting that at this concentration the total
272 amount of inhibitor may overcome the small amount of inducer emitted by the sub-
273 threshold ACTIVIN-bead. In conclusion, therefore, only Model B correctly predicts the
274 counterintuitive results of this experiment.

275 Taken together (Fig. 7) our results strongly favour a model by which cells assess their
276 status (in terms of whether or not they will constitute a primitive-streak-initiating centre)

277 in relation to the relative amounts of inducing and inhibiting signals they experience and
278 also in relation to the status of their neighbours, rather than by direct readout of the local
279 concentration of a morphogen that diffuses freely across the entire embryo.

280 Discussion

281 Here, we propose a “neighbourhood watch” model to explain how cells interpret
282 positional information to determine the site of gastrulation. Our present results, both from
283 computational modelling and experiments, strongly favour the idea that cells do not read
284 the concentrations of inducer and inhibitor (“SMAD-value”) locally and cell
285 autonomously, but rather interpret their own SMAD-value in relation to that of their
286 neighbours. Moreover, the results suggest that the distance over which such comparisons
287 take place is greater than just the immediately neighbouring cell on either side. In our
288 “neighbourhood watch” model, a neighbourhood size of 100-130 cells is predicted to
289 satisfy experimental observations.
290

291 In previous studies multiple mechanisms have been uncovered by which cells interpret
292 morphogen gradients. Can these other mechanisms explain our results? A key check when
293 answering this question is to ask whether an alternative mechanism can explain the lack of
294 ectopic streak and *cBRA* expression when an inducing signal is applied ectopically as a
295 broad domain (Fig. 2). The first possible mechanism is that cells respond directly to
296 morphogen concentration in a graded manner, as studied in explants of *Xenopus* embryos
297 with a bead graft (Gurdon et al., 1995). Another study using cultured blastula cells not
298 only supports this but also suggests that interaction with neighbouring cells is not required
299 for the interpretation of morphogen concentration (Gurdon et al., 1999). However, this
300 mechanism cannot explain our result of why a broad domain of inducer paradoxically
301 reduces ectopic *cBRA* expression. A second possible mechanism of morphogen
302 interpretation is one in which cells transform the signal concentration into the intracellular
303 activity of a transcription factor, generating dynamic gene expression patterns with
304 regulatory networks as shown for neural tube patterning (Cohen et al., 2013). This
305 mechanism explains well the precision of different thresholds for interpreting morphogen
306 concentrations based on duration and level (strength) of signals, which can be regulated by
307 exposure period to patterning signals as well as intracellular negative feedback by an
308 inhibitor. In our experiments using microbead grafts, however, the period of exposure and
309 the strength of signals were the same for all experiments (except where otherwise stated).
310 Specifically, our result that increasing the size of the domain exposed to inducing signal
311 reduces the incidence of ectopic *cBRA* expression suggests that spatial dynamics and cell-
312 cell communication are necessary in this system. These considerations make it more likely
313 that interactions between neighbouring cells are needed to position the primitive streak. A
314 recent paper proposes that a neighbourhood comparison of signal strength (called “spatial
315 fold change (SFC)” model) is required to position the determination front to regulate
316 somite size in the zebrafish trunk and tail bud (Simsek and Ozbudak, 2018), another
317 example of a large developing field undergoing patterning. This suggests that a
318 mechanism involving neighbourhood comparison for the interpretation of positional
319 information may be used by different systems, especially if they are of large size.

320 In the “neighbourhood watch” model in this study as well as in the SFC model (Simsek
321 and Ozbudak, 2018), cells adopt a relative or normalised value to be evaluated, rather than
322 the absolute morphogen concentration to assess their position. A relative value can
323 provide a stable response of cells to signals, promoting robustness and precision in signal

324 interpretation. Interestingly, a recent *in vitro* study suggests that cells sense relative signal
325 intensity in the TGF β /SMAD pathway as a fold-change value relative to background to
326 compensate for cellular noise (Frick et al., 2017).

327 How do cells communicate with their neighbours? In other words, by what mechanism
328 could cells assess their environment? In the wing imaginal disc of *Drosophila* embryos,
329 the TGF β -related protein Decapentaplegic (Dpp) acts as a morphogen conveying
330 positional information that results in positioning the wing veins and other features of the
331 wing. Signal-receiving cells have been shown to extend thin and long filopodia, called
332 cytonemes, which extend several cell diameters to the proximity of Dpp-producing cells
333 (Miller et al., 1995, Ramirez-Weber and Kornberg, 1999, Roy et al., 2011). It is worth
334 noting that the existence of very long filopodia extending very large distances (connecting
335 the invaginating archenteron with the future oral ectoderm at the opposite end of the
336 embryo) was observed by Gustafson and Wolpert in studies of gastrulation in the sea
337 urchin in 1961 (Gustafson and Wolpert, 1961) – this was one of the studies that initiated
338 thinking on pattern formation. As yet, these structures have not been observed in early
339 chick embryos, but this has not yet been investigated in detail. Another important question
340 is through what mechanism cells sense relative signals compared to their neighbours. As
341 we postulated in this study, one possible explanation is that cells evaluate the SMAD-
342 value, the relative strength of signals through competition of binding of these two
343 classes of SMADs (SMAD2/3 versus SMAD1/5/8) to the “co-SMAD”, SMAD4
344 (Candia et al., 1997). In this case, we cannot exclude the existence of a possible
345 intermediate messenger that can facilitate rapid sensing of the status of neighbouring
346 cells.

347 One question is whether the mechanism proposed here (involving only local cell
348 interactions and no long-range diffusion) is a feature unique to very large fields (several
349 mm), where meaningful positional information conveyed by diffusion alone is likely to be
350 impossible (Crick, 1970). There do appear to be several instances where diffusion of
351 informative morphogens is key, such as initial patterning of the *Drosophila* blastoderm
352 (Driever and Nusslein-Volhard, 1988a, Gregor et al., 2007b) and mesoderm induction by
353 activin in *Xenopus* animal caps (Gurdon et al., 1994, Gurdon et al., 1995, McDowell et al.,
354 1997). However, in the chick embryo, the anterior-posterior distance between the two
355 extremes of this ring should span about 300 cell lengths (in reality the marginal zone has a
356 thickness of about 120 μ m, corresponding to about 10 cells – here we represent it as being
357 one-cell-thick). As argued by Crick, it seems unlikely that this geometry can support the
358 formation or maintenance of long-range gradients of morphogens generated by free
359 diffusion (Crick, 1970). It therefore seems likely that positional information can be
360 imparted by a variety of different mechanisms, perhaps according to the size and
361 characteristics of the field to be patterned. It will be interesting to perform experiments
362 comparable to those in this paper in a system such as anterior-posterior patterning of the
363 chick limb, which is also large at early stages (HH18-20) and involves a localised
364 signalling region (the Zone of Polarizing Activity) (Riddle et al., 1993, Tickle et al.,
365 1975).

366 Here we propose that positional information (when interpreted by a collection of cells)
367 defines the location of the signalling centre (NODAL-expressing) that initiates primitive
368 streak formation (Bertocchini and Stern, 2002). Initiation of a streak can be seen as the
369 event that defines embryonic polarity. Our experiments and the associated models were
370 designed to ask questions about how cells within the marginal zone assess their positions
371 around the circumference of this signalling region, and thereafter determine the site next

372 to which (in the area pellucida) the primitive streak will start to form. However, it is
373 important to realise that in the embryo, the downstream consequence of these processes is
374 not only a spot of *cBRA* expression, but rather a true “streak”, gradually extending towards
375 the centre of the embryo. It has been shown previously that this elongation involves a
376 process of cell polarisation and intercalation affecting the same site in the area pellucida
377 where cells receive the inducing signals from the marginal zone (and which itself
378 expresses *cVG1* and *NODAL*) (Rozbicki et al., 2015, Voiculescu et al., 2007, Voiculescu
379 et al., 2014). Here, we observe cases where *cBRA* is induced but this is not followed by
380 formation of an elongated primitive streak. For example, this result is seen when three
381 beads are placed in the anterior marginal zone (A-B-A). One possible reason for this is
382 that the embryos were not incubated for long enough to allow the intercalation to take
383 place, but it is also possible that signals other than *cVG1* and inhibition of BMP are
384 required. Indeed it appears that non-canonical (planar cell polarity) WNT signalling drives
385 intercalation (Voiculescu et al., 2007) within the area pellucida. Whatever mechanisms
386 operate in the normal embryo to determine the site of primitive streak formation must
387 somehow coordinate these signalling events to generate the full structure.

388 Taken together, we provide evidence that in a large system with two opposing gradients,
389 cells assess their position in the field by measuring their location based on the relative
390 concentrations of the inducing (*cVG1/NODAL*) and inhibitory (BMP) signals, and this is
391 refined by taking cues from their local environment to assess the rate of change of these
392 signals locally. However, the gradients are unlikely to involve long-range diffusion of two
393 morphogens. Regulation of their strength is likely to involve other mechanisms resulting
394 in gradients of transcription and therefore rates of production of the factors.

395 **Materials and Methods**

396 *Embryo culture and wholemount in situ hybridisation*

397 Fertilised White Leghorn hens’ eggs (Henry Stewart, UK) were incubated for 2-4 hours to
398 obtain EGK X-XI embryos, which were then harvested in Pannett-Compton saline
399 (Pannett and Compton, 1924). After setting up for modified New culture (New, 1955,
400 Stern and Ireland, 1981), the cell pellets or beads were grafted as required for each
401 experiment, and the embryos cultured for the desired length of time before fixation in
402 formaldehyde. Whole mount in situ hybridisation was conducted as previously described
403 (Stern, 1998, Streit and Stern, 2001). The probes used were: *cVG1* (Shah et al., 1997),
404 *cBRA* (Kispert et al., 1995) and *BMP4* (Liem et al., 1995). Stained embryos were imaged
405 under an Olympus SZH10 stereomicroscope with a QImaging Retiga 2000R camera.
406 Some embryos were sectioned in sectioning at 10 μm .
407
408

409 *Misexpression of proteins with transfected cell pellets*

410 HEK293T cells were seeded at 5×10^5 cells/well in a 6-well dish and incubated for two
411 days (or 1×10^6 cells/well for transfection on the next day) at 37°C in a total of 2ml 10%
412 FBS DMEM (growth medium)/well. On the day of transfection, the growth medium was
413 changed to 1ml/well of 5% FBS DMEM (transfection medium) at least 30 min before
414 transfection. Transfection was carried out using PEI as reported previously (Papanayotou
415 et al., 2013). Briefly, 3 μl PEI (1mg/ml) was added for every 1 μg of DNA transfected, in
416 a total volume of 150 (for 0.5-2 μg)-200 μl (for 3-6 μg) DMEM in a sterile Eppendorf. 2 μg
417 DNA were transfected/well (containing 6 μl PEI/well). Expression plasmids were the
418 previously described DMVg1 (myc-tagged chimeric Vg1 containing the pro-domain of
419 Dorsalin; (Shah et al., 1997), pMT23 (murine BMP4; (Dickinson et al., 1990), and pCA β -
420 IRES-GFP (as a control). The latter was also used to estimate transfection efficiency.

421 Transfection mixtures were vortexed and then left for 10 minutes at room temperature for
422 the PEI/DNA to complex. The transfection mixture was then added dropwise to the
423 confluent monolayers of cells and incubated overnight at 37°C. The next day cells were
424 checked for transfection efficiency of the GFP plasmid; typically, efficiency ranged from
425 60-90%. Cells were washed three times with 1 X PBS, trypsinised and resuspended in a
426 total of 1.5ml growth medium and put into a sterile Eppendorf. The cell concentration was
427 estimated in a hemocytometer. A bulk cell suspension of the transfected cells was made in
428 the growth medium, so that each drop contained 500 cells in a total of 20µl growth
429 medium. Hanging drops were formed by placing the 20µl aliquots on the lid of a 6cm cell
430 culture dish, the bottom of which was filled with 5ml of sterile PBS or water to create a
431 humidified atmosphere. After placing several such aliquots well-spaced in a circle, the lid
432 was inverted and placed over the bottom of the dish, creating a mini culture chamber, to
433 allow the cells to coalesce into pellets without adhering to the plastic. Culture dishes were
434 incubated for 36-48 h at 37°C for the formation of pellets ranging in size from 500-1000
435 cells and used for grafts as required.

436 *Protein or chemical soaked microbeads*

437 Recombinant human BMP4 (R&D systems, 312-BP) was delivered using Affigel Blue
438 beads (BIO-RAD 1537302); recombinant human ACTIVIN A (R&D systems; 338-AC)
439 was delivered using Heparin-Acrylic beads (Sigma-Aldrich, H5236) and Dorsomorphin
440 hydrochloride (Tocris 3093) was loaded onto AG1X2-formate beads. In each case the
441 beads were incubated overnight at 4 °C in the desired concentration of protein or chemical.
442 Beads were washed in Pannett-Compton saline just before use.
443
444

445 *Encoding the biological problem mathematically*

446 The marginal zone is modelled as a one-dimensional ring of cells, comprising 600 cells in
447 total (based on the assumption that the embryo at this stage contains 20,000-50,000 cells
448 (Bertocchini and Stern, 2012) and on electron microscopy data (Lee et al., 2020,
449 Voiculescu et al., 2007) for estimates of cell size and the radius of the marginal zone).
450 Proxies for streak-inducer and -inhibitor concentrations are assigned to each cell i ,
451 represented as V_i and B_i respectively with $i = 1, \dots, 600$ (Fig. 3A).
452

453 Before the addition of beads, streak-inducer and -inhibitor levels are inferred from a
454 combination of RNAseq reads (Lee et al., 2020) and *in situ* hybridisation of *cVGI* and
455 *cBMP4* (Fig. S1A) respectively, at approximately stage EG&K XII. Inducer levels are
456 modelled using a gaussian function and inhibitor levels with a parabolic function (Fig.
457 S1B). The presence of a bead is modelled as having an additive (or subtractive) effect on
458 local protein concentration. The added values are constant for the width of the bead, and
459 then decrease exponentially in space. Therefore, placement of a bead invokes 4 parameters
460 (Fig. S4 A): the position of the centre of the bead, the width of the bead, the bead's
461 concentration (relating to magnitude of the added values, see Fig. S4 B) and the rate of
462 decay of the added compound in space (i.e. the 'spread' parameter of the exponential
463 distribution, see Fig. S4 C).
464

465 *Defining two models*

466 For each cell to make its decision to initiate streak formation, we define the relationship
467 between the amounts of SMAD2/3 (as a proxy for amount of inducer received) and
468 SMAD1/5/8 (as a proxy for amount of inhibitor received) within the cells. This is based
469 on the fact that inducing TGFβ-related signals (VG1/ACTIVIN/NODAL) act by

470 phosphorylation of SMAD2/3, whereas inhibitory TGF β -related signals (BMPs)
471 phosphorylate SMAD1/5/8 – cells have been proposed to evaluate the relative strength
472 of signals through competition of binding of these two classes of SMADs to the “co-
473 SMAD”, SMAD4 (Candia et al., 1997). Inducing and inhibitory SMADs compete to
474 form complexes with a fixed, limited amount of SMAD4. The inducer- and inhibitor-
475 linked SMAD complexes then move to the nucleus and regulate expression of different
476 target genes.

477
478 With V_i and B_i representing the levels of inducer- and inhibitor-linked SMAD
479 complexes in cell i respectively, we can then represent the total amount of SMAD4 in
480 a cell as the sum of the unbound, inducer-associated and inhibitor-associated SMAD4
481 ($1 + a_V V_i + a_B B_i$), where a_V and a_B are scalings of the protein concentrations. We then
482 represent the proportion of streak-inducing SMAD complex in a cell as

$$F_i = \frac{a_V V_i}{1 + a_V V_i + a_B B_i}. \quad (1)$$

483 F_i will hereafter be referred to as the “SMAD-value”, with higher values indicating
484 stronger induction.

485
486 We define two models for how cells interpret the SMAD-value to make the decision to
487 initiate a primitive streak.

488 A. Each cell compares its SMAD-values with a fixed threshold, without reference to
489 its neighbours. If the threshold is exceeded, the cell is defined to take part in
490 primitive streak initiation and will express *cBRA*. For each cell i , if

$$F_i > \alpha, \quad (2)$$

491 then that cell forms part of the primitive streak initiating domain.

492 B. Each cell compares its own SMAD-value with those of its neighbours. Each cell can
493 sense these values a certain distance away from itself and calculates an average
494 SMAD-value for all the neighbours it can see. If its own value is sufficiently large
495 compared to the average of its neighbours, the cell becomes part of a primitive streak
496 initiating centre, and expresses *cBRA*. Therefore, a streak is initiated next to cell i if

$$\frac{F_i - F_{\langle \text{nbhd} \rangle}}{F_i} > \beta, \quad (3)$$

497 where $F_{\langle \text{nbhd} \rangle}$ is defined to be the average value of F_j in a given neighbourhood
498 surrounding cell i . Specifically,

$$F_{\langle \text{nbhd} \rangle} = \frac{\sum_j F_j}{2n}, \quad (4)$$

499 with $j \in [i - n, i + n] \setminus \{i\}$, where $(2n + 1)$ is the full width of the neighbourhood.

500
501 Both Models A and B have as parameters a threshold value (α or β) and protein
502 concentration scalings (a_V and a_B). Additionally, Model B requires the size of the
503 neighbourhood (n) to be defined as a parameter.

504 *Parameter inference*

505
506 For the final stage of the modelling process, we ask whether there exists a set of
507 parameters allowing each model to replicate a target result. As both models invoke many
508 parameters, resulting in a large and high-dimensional parameter space, we automate the
509 search with a MCMC Bayesian computation algorithm. Parameter values are scored using
510 a likelihood function which quantifies how well model predictions match a target result.

511 The target result is defined based upon an experimental result (Fig. 3 and Fig. S4) or a
512 new possible theory (Figs. 4-6).

513
514 For the parameter search, we fix the expected width of the streak initiating domain, as well
515 as the positions and widths of the beads. We allow the concentration and spread
516 parameters of the beads to vary (denoted c and s) in addition to all model parameters (α , β ,
517 a_V , a_B , n). Uniform prior distributions are defined for all parameters except the protein
518 concentration scalings, a_V and a_B . For these parameters we define $b_V = \log_{10} a_V$ and
519 $b_B = \log_{10} a_B$, which are then uniformly distributed. We define biologically plausible
520 ranges within which parameters are allowed to vary (shown in Fig. S6).

521
522 In order to obtain the likelihood function, we first define for each cell, the distance (f_i) of
523 the SMAD-value (F_i) to the threshold for streak formation, which for Model A is

$$f_i^{(A)} = F_i - \alpha, \quad (5)$$

524 and for Model B

$$f_i^{(B)} = \frac{F_i - F_{\langle \text{nbhd} \rangle}}{F_i} - \beta. \quad (6)$$

525 So $f_i > 0$ implies that a streak will form in cell i , and $f_i \leq 0$ implies no streak will form.
526 For convenience we can write that $f_i = f_i(\theta)$ where $\theta = \{\alpha, \beta, a_V, a_B, n, c, s\}$, the set of
527 parameters to be varied.

528
529 The target result is encoded as a binary decision for each cell: presence or absence of
530 *cBRA* expression indicating the site of primitive streak formation. We therefore define

$$D_i = \begin{cases} 1, & \text{where streak is hypothesised in cell } i, \\ -1, & \text{where no streak is hypothesised in cell } i. \end{cases} \quad (7)$$

531
532 Then the ‘likelihood’ of parameters θ can be calculated as

$$\mathcal{L}_i(\theta) \sim \frac{1}{2} \left[1 + \tanh \left(\frac{D_i f_i(\theta)}{\Delta} \right) \right], \quad (8)$$

533 in cell i , which approximates a step function as $\Delta \rightarrow 0$ (Fig. S5). For all parameter
534 searches, we use $\Delta = 0.05$. The likelihood is calculated individually for each cell of each
535 experimental design given to the algorithm. The product of the likelihoods (across cells,
536 designs and parameters) is calculated giving the total likelihood for a given set of
537 parameter values. The parameters used to calculate the total likelihood include all model
538 parameters and the bead parameters relevant for the experiment. Only cells in the anterior
539 half of the embryo are used to calculate the total likelihood, because beads are only
540 grafted anteriorly in the experiments modelled. As a result of this, Model B does not
541 always predict the presence of an endogenous streak next to the posterior margin.

542
543 The posterior distributions of the parameters were obtained via the MCMC Bayesian
544 computation in the pyDREAM package (Shockley et al., 2017) which implements a
545 DREAM_(ZS) algorithm (Laloy and Vrugt, 2012). The algorithm was run using 5 Markov
546 chains for a minimum of 5000 iterations per chain, and convergence was tested using the
547 Gelman–Rubin statistic (Gelman and Rubin, 1992, Brooks and Gelman, 1998). The
548 posterior distributions are shown in Figure S6.

549
550 The Bayesian computation algorithm maximises the likelihood (equation 8), quickly and
551 efficiently finding sets of parameter values minimizing the distance between the target

552 result (D_i) and the model result (f_i). Specifically, the likelihood function is defined so as to
553 strongly favour sets of parameters where D_i and f_i have the same sign (i.e. both above zero
554 or both below zero). Occasionally this means that parameter values obtained by the
555 algorithm give model values close to, but not exceeding, the threshold and therefore do
556 not predict ectopic streaks as required by the target result. Therefore, all parameter values
557 found using the Bayesian computation algorithm were checked to ensure that ectopic
558 streaks were predicted in locations dictated by the target result. This was done by
559 verifying that at least one cell exceeded the threshold to produce an ectopic streak in the
560 expected location (i.e. the location of a bead). Thus, if parameter values for a given model
561 allowed the prediction of correct ectopic streak placement, these values were deemed to
562 give ‘success’ for a specific experimental design. The parameter values used in the plots in
563 Figures 3-6 and S3 were chosen to maximise both the success rate and the likelihood. All
564 parameter values are given in Data S1.

566 The parameter search is performed for each group of experimental designs comprising
567 Figures 1, 2, 4/5 and 6. Ideally, the parameter search must output a single set of bead
568 parameters, allowing both models to approximate the target results as closely as possible
569 (Fig. 3 H). However, this acts as a restriction that might limit the ability of either model to
570 replicate the target result. Therefore, the parameter search was also performed with all
571 parameters varying for both models independently removing this restriction (Fig. 3 I). We
572 verified that seeking a single set of bead parameters did not reduce the ability of either
573 model to replicate the target result (Fig. 3 J).

574 **Author contributions:** HCL conducted all embryo experiments; CH designed the models
575 and implemented them; NMMO constructed the vectors and performed cell culture; RPC
576 and KP provided advice and ideas on mathematical methods; LW provided inspiration and
577 stimulated questions during the early stages of the study; CDS supervised the study. HCL,
578 CH and CDS wrote the paper.

581 **Competing interests:** The authors declare no competing interests.

582 **Funding:** This research was supported by Basic Science Research Program through the
583 National Research Foundation of Korea (NRF) funded by the Ministry of Education
584 (2014R1A6A3A03053468) to HCL, by an MRC DTP studentship (MR/N013867/1) to CH
585 and by a Wellcome Trust Investigator Award (107055/Z/15/Z) to CDS.

587 **Data and materials availability:** The software used for the mathematical and
588 computational modelling is available at [https://github.com/catoHaste/Neighbourhood-](https://github.com/catoHaste/Neighbourhood-streak)
589 [streak](https://github.com/catoHaste/Neighbourhood-streak).

591 **References.**

- 592 ARIAS, C. F., HERRERO, M. A., STERN, C. D. & BERTOCCHINI, F. 2017. A molecular
593 mechanism of symmetry breaking in the early chick embryo. *Sci Rep*, 7, 15776.
594 BERTOCCHINI, F., SKROMNE, I., WOLPERT, L. & STERN, C. D. 2004. Determination of
595 embryonic polarity in a regulative system: evidence for endogenous inhibitors acting
596 sequentially during primitive streak formation in the chick embryo. *Development*, 131,
597 3381-90.
598 BERTOCCHINI, F. & STERN, C. D. 2002. The hypoblast of the chick embryo positions the
599 primitive streak by antagonizing nodal signaling. *Dev Cell*, 3, 735-44.

- 501 BERTOCCHINI, F. & STERN, C. D. 2012. Gata2 provides an early anterior bias and uncovers a
502 global positioning system for polarity in the amniote embryo. *Development*, 139, 4232-8.
- 503 BODE, H. 2011. Axis formation in hydra. *Annu Rev Genet*, 45, 105-17.
- 504 BROOKS, S. P. & GELMAN, A. 1998. General Methods for Monitoring Convergence of
505 Iterative Simulations. *Journal of Computational and Graphical Statistics*, 7, 434-455.
- 506 CANDIA, A. F., WATABE, T., HAWLEY, S. H., ONICHTCHOUK, D., ZHANG, Y.,
507 DERYNCK, R., NIEHRS, C. & CHO, K. W. 1997. Cellular interpretation of multiple
508 TGF-beta signals: intracellular antagonism between activin/BVg1 and BMP-2/4 signaling
509 mediated by Smads. *Development*, 124, 4467-80.
- 510 COHEN, M., BRISCOE, J. & BLASSBERG, R. 2013. Morphogen interpretation: the
511 transcriptional logic of neural tube patterning. *Curr Opin Genet Dev*, 23, 423-8.
- 512 CRICK, F. 1970. Diffusion in embryogenesis. *Nature*, 225, 420-2.
- 513 DESSAUD, E., RIBES, V., BALASKAS, N., YANG, L. L., PIERANI, A., KICHEVA, A.,
514 NOVITCH, B. G., BRISCOE, J. & SASAI, N. 2010. Dynamic assignment and
515 maintenance of positional identity in the ventral neural tube by the morphogen sonic
516 hedgehog. *PLoS Biol*, 8, e1000382.
- 517 DICKINSON, M. E., KOBRIN, M. S., SILAN, C. M., KINGSLEY, D. M., JUSTICE, M. J.,
518 MILLER, D. A., CECI, J. D., LOCK, L. F., LEE, A., BUCHBERG, A. M. & ET AL.
519 1990. Chromosomal localization of seven members of the murine TGF-beta superfamily
520 suggests close linkage to several morphogenetic mutant loci. *Genomics*, 6, 505-20.
- 521 DRIEVER, W. & NUSSLEIN-VOLHARD, C. 1988a. The bicoid protein determines position in
522 the Drosophila embryo in a concentration-dependent manner. *Cell*, 54, 95-104.
- 523 DRIEVER, W. & NUSSLEIN-VOLHARD, C. 1988b. A gradient of bicoid protein in Drosophila
524 embryos. *Cell*, 54, 83-93.
- 525 FRICK, C. L., YARKA, C., NUNNS, H. & GOENTORO, L. 2017. Sensing relative signal in the
526 Tgf-beta/Smad pathway. *Proc Natl Acad Sci U S A*, 114, E2975-E2982.
- 527 GELMAN, A. & RUBIN, D. B. 1992. Inference from Iterative Simulation Using Multiple
528 Sequences. *Statistical Science*, 7, 457-472.
- 529 GREEN, J. B. & SMITH, J. C. 1990. Graded changes in dose of a Xenopus activin A homologue
530 elicit stepwise transitions in embryonic cell fate. *Nature*, 347, 391-4.
- 531 GREGOR, T., TANK, D. W., WIESCHAUS, E. F. & BIALEK, W. 2007a. Probing the limits to
532 positional information. *Cell*, 130, 153-64.
- 533 GREGOR, T., WIESCHAUS, E. F., MCGREGOR, A. P., BIALEK, W. & TANK, D. W. 2007b.
534 Stability and nuclear dynamics of the bicoid morphogen gradient. *Cell*, 130, 141-52.
- 535 GURDON, J. B., HARGER, P., MITCHELL, A. & LEMAIRE, P. 1994. Activin signalling and
536 response to a morphogen gradient. *Nature*, 371, 487-92.
- 537 GURDON, J. B., MITCHELL, A. & MAHONY, D. 1995. Direct and continuous assessment by
538 cells of their position in a morphogen gradient. *Nature*, 376, 520-1.
- 539 GURDON, J. B., STANDLEY, H., DYSON, S., BUTLER, K., LANGON, T., RYAN, K.,
540 STENNARD, F., SHIMIZU, K. & ZORN, A. 1999. Single cells can sense their position in
541 a morphogen gradient. *Development*, 126, 5309-17.
- 542 GUSTAFSON, T. & WOLPERT, L. 1961. Studies on the cellular basis of morphogenesis in the
543 sea urchin embryo. Gastrulation in vegetalized larvae. *Exp Cell Res*, 22, 437-49.
- 544 KISPERT, A., ORTNER, H., COOKE, J. & HERRMANN, B. G. 1995. The chick Brachyury
545 gene: developmental expression pattern and response to axial induction by localized
546 activin. *Dev Biol*, 168, 406-15.
- 547 KUMAR, A., GATES, P. B. & BROCKES, J. P. 2007. Positional identity of adult stem cells in
548 salamander limb regeneration. *C R Biol*, 330, 485-90.

- 549 LALOY, E. & VRUGT, J. A. 2012. High-dimensional posterior exploration of hydrologic models
550 using multiple-try DREAM(ZS) and high-performance computing. *Water Resources*
551 *Research*, 48.
- 552 LECUIT, T., BROOK, W. J., NG, M., CALLEJA, M., SUN, H. & COHEN, S. M. 1996. Two
553 distinct mechanisms for long-range patterning by Decapentaplegic in the Drosophila wing.
554 *Nature*, 381, 387-393.
- 555 LEE, H. C., LU, H. C., TURMAINE, M., OLIVEIRA, N. M. M., YANG, Y., DE ALMEIDA, I.
556 & STERN, C. D. 2020. Molecular anatomy of the pre-primitive-streak chick embryo.
557 *Open Biol*, 10, 190299.
- 558 LIEM, K. F., JR., TREMML, G., ROELINK, H. & JESSELL, T. M. 1995. Dorsal differentiation
559 of neural plate cells induced by BMP-mediated signals from epidermal ectoderm. *Cell*, 82,
560 969-79.
- 561 MCDOWELL, N., ZORN, A. M., CREASE, D. J. & GURDON, J. B. 1997. Activin has direct
562 long-range signalling activity and can form a concentration gradient by diffusion. *Curr*
563 *Biol*, 7, 671-81.
- 564 MILLER, J., FRASER, S. E. & MCCLAY, D. 1995. Dynamics of thin filopodia during sea urchin
565 gastrulation. *Development*, 121, 2501-11.
- 566 MITRANI, E., ZIV, T., THOMSEN, G., SHIMONI, Y., MELTON, D. A. & BRIL, A. 1990.
567 Activin can induce the formation of axial structures and is expressed in the hypoblast of
568 the chick. *Cell*, 63, 495-501.
- 569 NEW, D. A. T. 1955. A new technique for the cultivation of the chick embryo in vitro. *J.*
570 *Embryol. exp. Morph.*, 3, 326-331.
- 571 PANNETT, C. A. & COMPTON, A. 1924. The cultivation of tissues in saline embryonic juice.
572 *Lancet*, 1, 381-384.
- 573 PAPANAYOTOU, C., DE ALMEIDA, I., LIAO, P., OLIVEIRA, N. M., LU, S. Q.,
574 KOUGIOUMTZIDOU, E., ZHU, L., SHAW, A., SHENG, G., STREIT, A., YU, D.,
575 WAH SOONG, T. & STERN, C. D. 2013. Calfacilitin is a calcium channel modulator
576 essential for initiation of neural plate development. *Nat Commun*, 4, 1837.
- 577 POSTLETHWAIT, J. H. & SCHNEIDERMAN, H. A. 1971. Pattern formation and determination
578 in the antenna of the homoeotic mutant Antennapedia of Drosophila melanogaster. *Dev*
579 *Biol*, 25, 606-40.
- 580 RAMIREZ-WEBER, F. A. & KORNBERG, T. B. 1999. Cytonemes: cellular processes that
581 project to the principal signaling center in Drosophila imaginal discs. *Cell*, 97, 599-607.
- 582 RIDDLE, R. D., JOHNSON, R. L., LAUFER, E. & TABIN, C. 1993. Sonic hedgehog mediates
583 the polarizing activity of the ZPA. *Cell*, 75, 1401-16.
- 584 ROY, S., HSIUNG, F. & KORNBERG, T. B. 2011. Specificity of Drosophila cytonemes for
585 distinct signaling pathways. *Science*, 332, 354-8.
- 586 ROZBICKI, E., CHUAI, M., KARJALAINEN, A. I., SONG, F., SANG, H. M., MARTIN, R.,
587 KNOLKER, H. J., MACDONALD, M. P. & WEIJER, C. J. 2015. Myosin-II-mediated
588 cell shape changes and cell intercalation contribute to primitive streak formation. *Nat Cell*
589 *Biol*, 17, 397-408.
- 590 SCHALLER, H. C. 1973. Isolation and characterization of a low-molecular-weight substance
591 activating head and bud formation in hydra. *J Embryol Exp Morphol*, 29, 27-38.
- 592 SHAH, S. B., SKROMNE, I., HUME, C. R., KESSLER, D. S., LEE, K. J., STERN, C. D. &
593 DODD, J. 1997. Misexpression of chick Vg1 in the marginal zone induces primitive
594 streak formation. *Development*, 124, 5127-38.
- 595 SHOCKLEY, E. M., VRUGT, J. A. & LOPEZ, C. F. 2017. PyDREAM: high-dimensional
596 parameter inference for biological models in python. *Bioinformatics*, 34, 695-697.

- 597 SIMSEK, M. F. & OZBUDAK, E. M. 2018. Spatial Fold Change of FGF Signaling Encodes
598 Positional Information for Segmental Determination in Zebrafish. *Cell Rep*, 24, 66-78 e8.
- 599 SKROMNE, I. & STERN, C. D. 2002. A hierarchy of gene expression accompanying induction
700 of the primitive streak by Vg1 in the chick embryo. *Mech Dev*, 114, 115-8.
- 701 STERN, C. D. 1998. Detection of multiple gene products simultaneously by in situ hybridization
702 and immunohistochemistry in whole mounts of avian embryos. *Curr Top Dev Biol*, 36,
703 223-243.
- 704 STERN, C. D. & IRELAND, G. W. 1981. An integrated experimental study of endoderm
705 formation in avian embryos. *Anat Embryol*, 163, 245-63.
- 706 STERN, C. D., YU, R. T., KAKIZUKA, A., KINTNER, C. R., MATHEWS, L. S., VALE, W.
707 W., EVANS, R. M. & UMESONO, K. 1995. Activin and its receptors during gastrulation
708 and the later phases of mesoderm development in the chick embryo. *Dev Biol*, 172, 192-
709 205.
- 710 STREIT, A., LEE, K. J., WOO, I., ROBERTS, C., JESSELL, T. M. & STERN, C. D. 1998.
711 Chordin regulates primitive streak development and the stability of induced neural cells,
712 but is not sufficient for neural induction in the chick embryo. *Development*, 125, 507-19.
- 713 STREIT, A. & STERN, C. D. 1999. Mesoderm patterning and somite formation during node
714 regression: differential effects of chordin and noggin. *Mech Dev*, 85, 85-96.
- 715 STREIT, A. & STERN, C. D. 2001. Combined whole-mount in situ hybridization and
716 immunohistochemistry in avian embryos. *Methods*, 23, 339-44.
- 717 TICKLE, C., SUMMERBELL, D. & WOLPERT, L. 1975. Positional signalling and specification
718 of digits in chick limb morphogenesis. *Nature*, 254, 199-202.
- 719 TORLOPP, A., KHAN, M. A., OLIVEIRA, N. M., LEKK, I., SOTO-JIMENEZ, L. M.,
720 SOSINSKY, A. & STERN, C. D. 2014. The transcription factor Pitx2 positions the
721 embryonic axis and regulates twinning. *Elife*, 3, e03743.
- 722 VOICULESCU, O., BERTOCCHINI, F., WOLPERT, L., KELLER, R. E. & STERN, C. D. 2007.
723 The amniote primitive streak is defined by epithelial cell intercalation before gastrulation.
724 *Nature*, 449, 1049-52.
- 725 VOICULESCU, O., BODENSTEIN, L., LAU, I. J. & STERN, C. D. 2014. Local cell interactions
726 and self-amplifying individual cell ingression drive amniote gastrulation. *Elife*, 3, e01817.
- 727 WOLPERT, L. 1968. The French flag problem: a contribution to the discussion on pattern
728 development and regeneration. In: WADDINGTON, C. H. (ed.) *Towards a Theoretical*
729 *Biology*. Aldine Publishing Co.
- 730 WOLPERT, L. 1969. Positional information and the spatial pattern of cellular differentiation.
731 *Journal of Theoretical Biology*, 25, 1-47.
- 732 YU, P. B., HONG, C. C., SACHIDANANDAN, C., BABITT, J. L., DENG, D. Y., HOYNG, S.
733 A., LIN, H. Y., BLOCH, K. D. & PETERSON, R. T. 2008. Dorsomorphin inhibits BMP
734 signals required for embryogenesis and iron metabolism. *Nat Chem Biol*, 4, 33-41.

735 736 737 738 739 **Figure Legends**

740
741 **Fig. 1. Interruption of a domain exposed to an inducing signal increases the incidence**
742 **of primitive streak induction – experiments with secreting cells. (A, B)** When
743 two pellets of cVG1-expressing cells are grafted in the anterior marginal zone
744 (aMZ), only a single ectopic primitive streak (red arrow) is generated. **(C, D)**
745 Control cell pellets do not induce a streak. **(E-G)** Experimental design. Ectopic

746 streak formation is checked in three different conditions: misexpression of *cVg1*
747 in a wide area using four *cVg1*-expressing cell pellets (**E**), introduction of a
748 ‘spacer’ (control cell pellet) to interrupt a set of four *cVg1* pellets (**F**), and
749 introduction of an inhibitor (BMP4-expressing cell pellet) to interrupt a set of four
750 *cVg1* inducing pellets (**G**). (**H-J**) representative embryos for each experiment. The
751 frequency of primitive streak formation is enhanced by interrupting the domain of
752 inducing signal, even when this interruption is achieved by introduction of an
753 inhibitor (**J**). (**K**) Summary graph showing the incidence of each type of result for
754 the above experiments (**E-J**). PS: primitive streak. Black and red arrows,
755 endogenous and ectopic streaks, respectively. Dotted lines, position of the cell
756 pellets. *cBRA*, primitive streak marker.

757
758 **Fig. 2. Interruption of a domain exposed to an inducing signal increases the incidence**
759 **of primitive streak induction – experiments with protein-soaked beads. (A-E)**
760 Experimental design. Induction of a streak is assessed after five combinations of
761 bead grafts: 3 control beads (**A**), An ACTIVIN-soaked bead flanked by control
762 beads (**B**), exposing a wide area to the inducing signal by grafting 3 ACTIVIN-
763 soaked beads (**C**), interrupting the inducing signal by adding a ‘space’ (control
764 bead) to separate two adjacent inducing (ACTIVIN) beads (**D**), and adding an
765 inhibitor (BMP4-soaked bead) to separate two adjacent ACTIVIN beads (**E**). (**F-J**)
766 Representative embryos for each experiment. Two primitive streaks only form
767 when the inducing signal is interrupted, even when adding an inhibitory signal. (**K**)
768 Summary graph showing the incidence of each type of result for the above
769 experiments. Note that a higher concentration of BMP4 (25 ng/μl), does not allow
770 an ectopic streak to form. Dotted circles, location of beads. Other abbreviations
771 and symbols as in Fig. 1.

772
773 **Fig. 3. Mathematical model and verification *in silico*. (A-B) Model workflow. (A)** The
774 dotted line represents the marginal zone. Concentrations of primitive-streak-
775 inducing and -inhibiting proteins are inferred from experimental design. Target site
776 of streak initiation is encoded for comparison with model predictions. (**B**) In each
777 cell, both models weigh concentrations of streak-inducing and -inhibiting proteins.
778 Model A assumes that cells act autonomously to define the site of streak
779 formation. Model B assumes that cells compare concentrations within a given
780 neighbourhood to initiate streak formation. Model values are plotted for the entire
781 embryo, where values above a threshold define the site of streak initiation. (**C-G**)
782 *In silico* simulations of bead experiments in Figure 2. Top, experimental designs.
783 First row of plots: inducer levels shown as a red line, inhibitor in blue; the lower
784 bar marks the expected position of streak initiation. Second row of plots: Model A
785 values and corresponding predicted streak locations. Third row: Model B values
786 and streak locations. (**C, E-G**) A model is defined as “successful” for one
787 experimental design if the predicted number and location of streaks matches the
788 target result. (**D**) Model A fails to replicate the experimental result. No parameter
789 values are found where Model A is successful for both designs (**C**) and (**D**). (**E-G**)
790 Unlike Model A, Model B predicts that exchanging the control bead for a bead of
791 low dose inhibitor will counter-intuitively increase the chances of ectopic streak
792 formation (insets). (**H-J**) To ensure that finding a single set of parameters does not
793 limit the ability of either model to replicate the target results, we used two
794 approaches for parameter estimation: (**H**) a single set of bead parameters is defined

795 for both models, or **(I)** bead and model parameters vary freely for both models,
796 allowing the maximum chance of success. **(J)** approach H does not reduce the
797 success rate of either model. Model B outperforms Model A in all cases.

798 **Fig. 4. Decreasing the amount of inhibitor induces ectopic primitive streak**
799 **formation.** Local repression of inhibitor (BMP) using Dorsomorphin induces a
800 streak both *in silico* and *in vivo*. **(A)** Experimental setup. **(B)** Results of *in silico*
801 simulations (colours and other conventions as in Fig. 3). Both models predict
802 ectopic primitive streak formation when the concentration of inhibitor is decreased
803 locally. **(C-F)** Results of *in vivo* experiments. A graft of a 1mM Dorsomorphin-
804 soaked bead in the anterior marginal zone induces formation of an ectopic streak
805 expressing *cBRA* after overnight culture **(C, arrow)**, which is preceded (at 6 h) by
806 ectopic expression of *cVGI* **(E, arrow)**. Control (0.2% DMSO) beads have no
807 effect **(D, F)**. Dotted circles, location of microbeads. The proportion of embryos
808 showing the phenotype illustrated are indicated in the lower right of each panel.

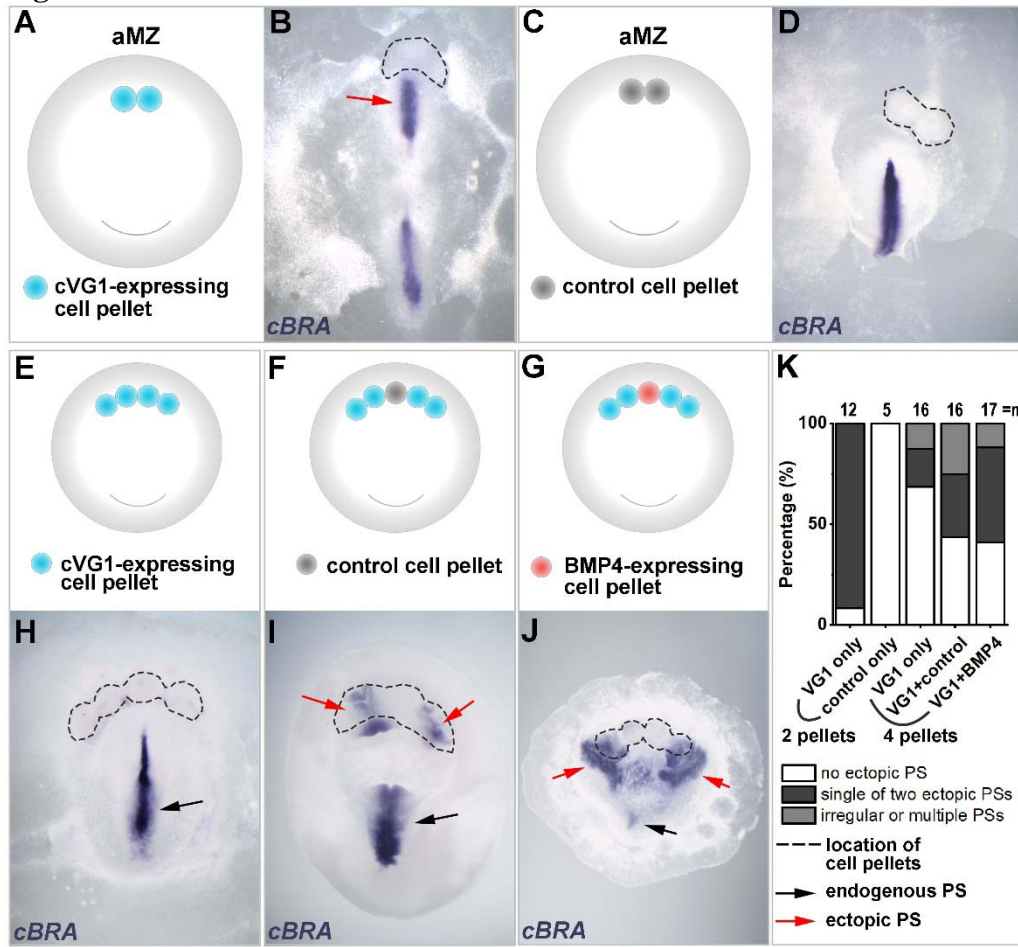
809
810 **Fig. 5. Increasing the amount of inhibitor augments the streak-inducer.** Local
811 overexpression of inhibitor (BMP4) increases streak-inducing values *in silico*, and
812 *cVGI* expression *in vivo* in neighbouring cells. **(A)** Experimental setup. **(B)** Results
813 of *in silico* simulations. Only Model B predicts an increase in streak-inducing
814 value in cells neighbouring the bead of inhibitor (arrowheads), but at levels
815 insufficient to initiate an ectopic streak. **(C-G)** Results of *in vivo* experiments. No
816 ectopic primitive streak (marked by *cBRA*) is induced overnight after a graft of
817 BMP4 (50 ng/μl) soaked bead **(C)**. However, a short time (4.5 h) after grafting,
818 ectopic *cVGI* expression is induced in the marginal zone **(D)** in neighbouring cells
819 **(F)** but not in the cells lying directly above the bead **(F, square bracket)**. By 6 h
820 after grafting, induced *cVGI* expression is no longer visible in the marginal zone,
821 remaining only in the extraembryonic endoderm (germ wall) **(E, arrow and G)**.
822 The dashed lines in **(D and E)** indicate the level of the sections in **(F and G)**.
823 Dotted circles, location of microbeads. The proportion of embryos showing the
824 illustrated phenotypes is indicated on the lower right of each panel. Orientation of
825 sections (in F and G): left-to-right is dorsal-to-ventral. Scale bar for **(F and G)**,
826 100 μm.

827
828 **Fig. 6. Challenging the models: effect of placing an inhibitor next to sub-threshold**
829 **amounts of inducer.** **(A-C)** Experimental design. Three conditions were tested:
830 two BMP4 beads (6.25 ng/μl) **(B)** separated by a control bead **(C)** **(A)**, a bead
831 loaded with sub-threshold (2.5 ng/μl) amounts of ACTIVIN **(A)** flanked by two
832 control beads **(C)** **(B)** and a sub-threshold bead of activin flanked by two beads of
833 inhibitor (BMP4) **(C)**. **(D-F)** Results of *in silico* simulations. Only Model B
834 predicts that introducing a sub-threshold amount of inducer flanked by beads of
835 inhibitor will paradoxically generate a site of ectopic PS formation. **(G-I)** Results
836 of *in vitro* experiments showing representative embryos for each experiment.
837 Number of embryos showing the phenotypes are indicated in each panel. *In vivo*,
838 grafting a sub-threshold ACTIVIN bead flanked by two BMP4 beads in the
839 marginal zone can induce ectopic *cBRA* expression **(I)**. No such induction is seen
840 in the other combinations (B-C-B or C-A-C) **(A, B, G, H)**. Black and red arrows:
841 endogenous and ectopic *cBRA* expression, respectively. Dotted circles: location of
842 microbeads. The numbers on the lower right of panels G-I indicate the frequency
843 of the illustrated result for each experimental combination.

344
345 **Fig. 7. A “neighbourhood watch” model accounts for positioning the site where**
346 **primitive streak formation is initiated in the marginal zone of the early chick**
347 **embryo. (A-B)** The “SMAD-value” represents a combination of inducing and
348 inhibiting signals. Cells assess their position by comparing their SMAD-value with
349 those of their neighbours. Blue: territory over which cells are able to sense. Purple:
350 cell(s) initiating primitive streak formation. Light purple: partial/weak
351 induction. **(A)** The domain of induction must be sufficiently narrow for cells to
352 sense a local maximum. When a local maximum is located, primitive streak
353 formation is initiated in the marginal zone. **(B)** Cells adjacent to a domain of
354 inhibition detect their relatively high SMAD-value and react by emitting streak-
355 inducing signals (cVG1). However, the induction is not sufficiently strong to
356 initiate the formation of a full streak (no *cBRA* expression). **(C)** Comparison of
357 predictions by two models: one (“threshold only”) where positional information is
358 interpreted cell-autonomously solely by assessing the morphogen concentrations,
359 and another (“neighbourhood watch”) where cells make local comparisons with
360 their neighbours to assess their position in the gradients. First row: a narrow
361 domain of induction results in initiation of primitive streak formation. Second row:
362 broadening the domain of induction distinguishes between the two models. The
363 “neighbourhood watch” model predicts that streak formation will not be initiated,
364 matching experimental data. Third row: a sub-threshold amount of inducer results
365 in no ectopic *cBRA* expression. Fourth row, the “threshold only” model predicts
366 that adding inhibitor adjacent to a sub-threshold amount of inducer will either have
367 no effect or reduce the chance of ectopic streak formation. In contrast, the
368 “neighbourhood watch” model correctly predicts the counter-intuitive result that
369 addition of inhibitor increases the chances of ectopic streak initiation. Green ticks
370 and red crosses represent whether the model prediction matches the experimental
371 data or not, respectively. Dashed and dotted lines represent thresholds for
372 interpretation of morphogen concentration. Purple: primitive streak formation
373 initiated in cells above threshold.
374

375

Fig. 1

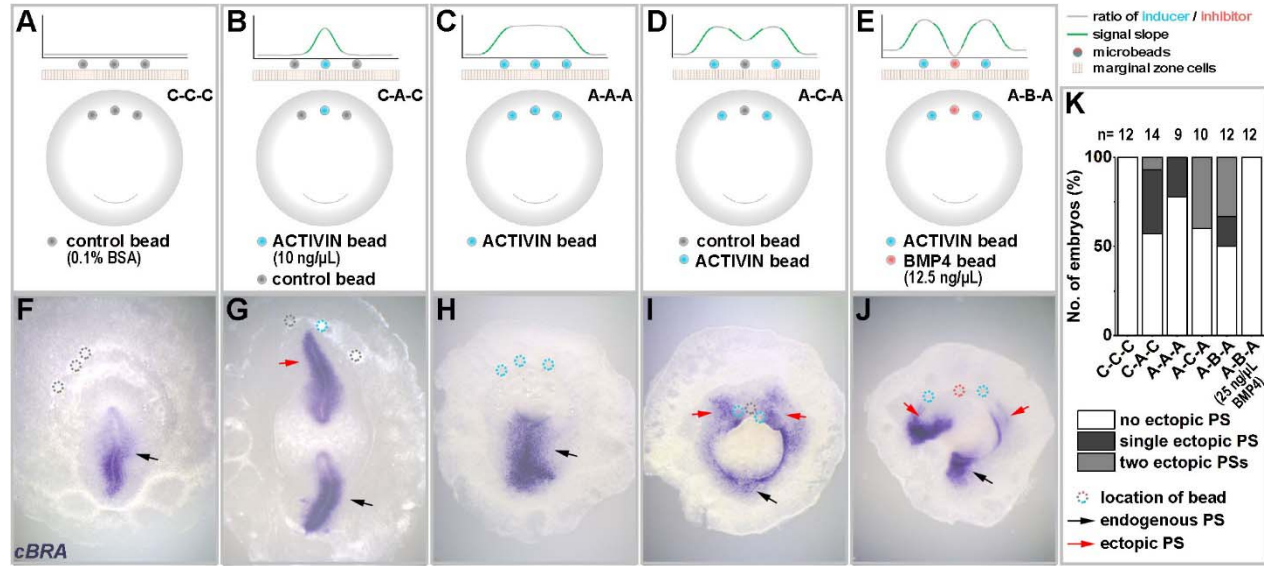


376

377

378

Fig. 2

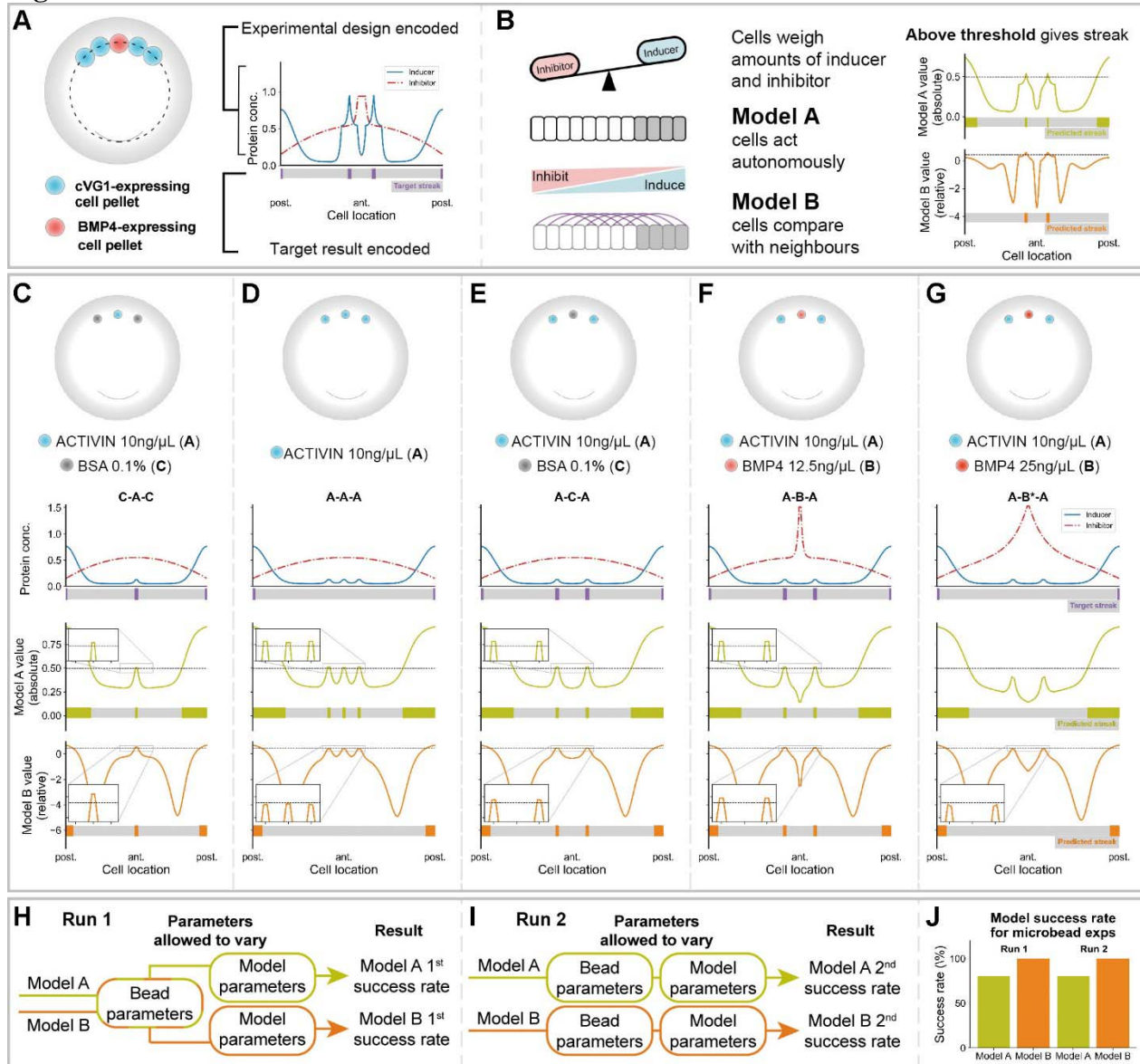


379

380

381

Fig. 3

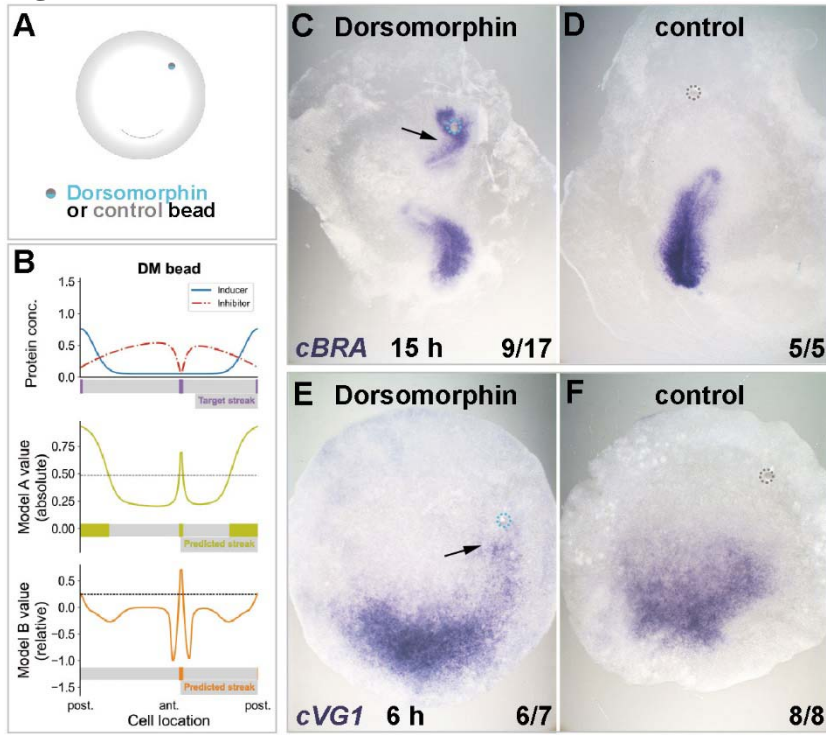


382

383

384

Fig. 4

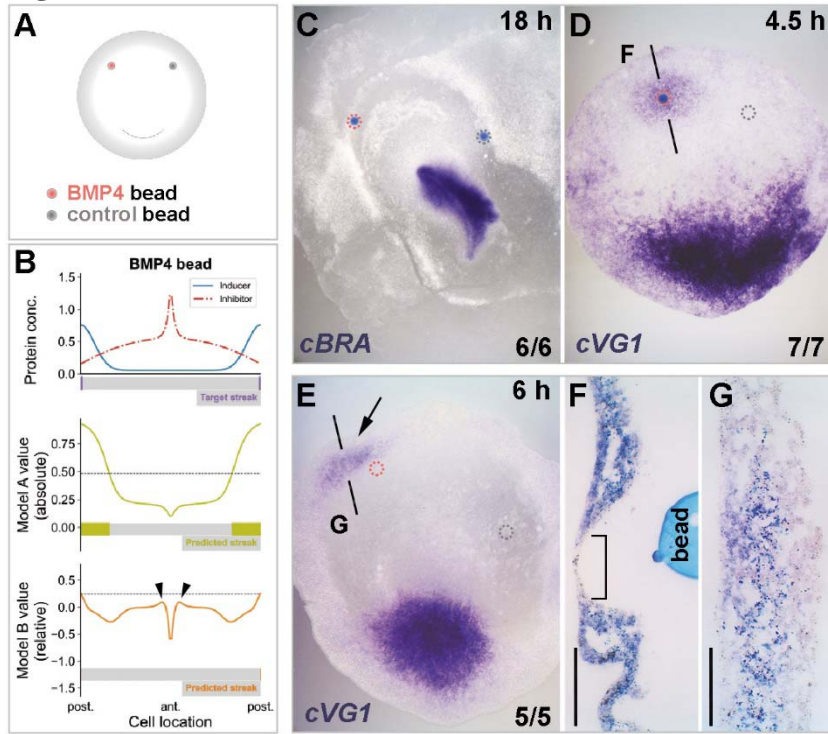


385

386

387

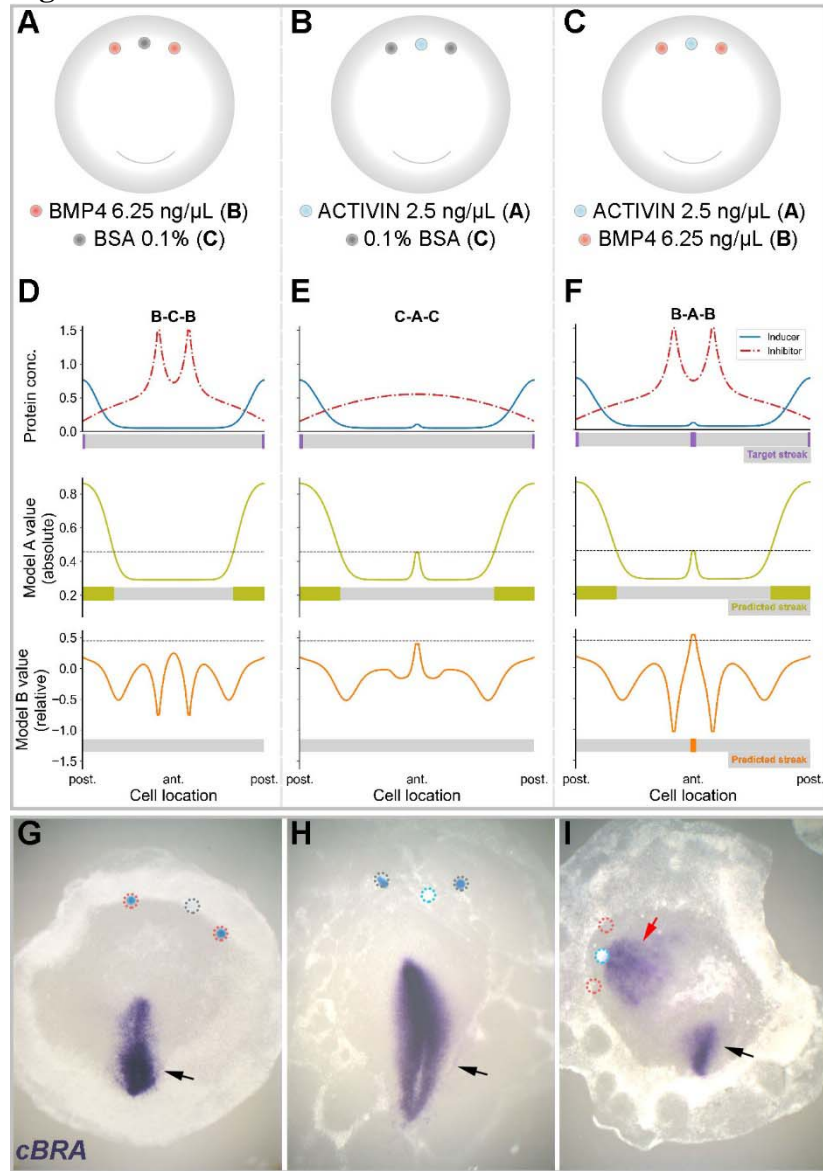
Fig. 5



388
389

390

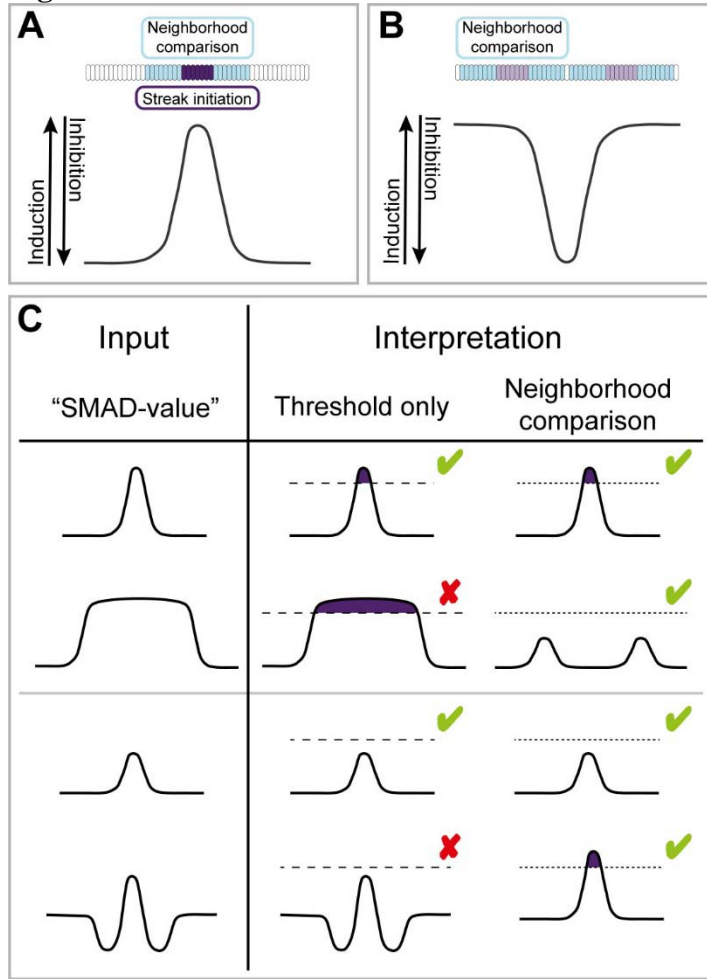
Fig. 6



391
392

393

Fig. 7



394
395